

Novel Results on the Large-Signal Dynamic Admittance of $p-n$ -Junctions

Edval J. P. Santos and Anatoly A. Barybin*

Laboratory for Devices and Nanostructures at the Departamento de Eletrônica e Sistemas, Universidade Federal de Pernambuco, 50740-530, Recife, Brazil. E-mail: edval@ee.ufpe.br .

() Electronics Department, Saint-Petersburg Electrotechnical University, 197376, Saint-Petersburg, Russia, on leave at the Departamento de Eletrônica e Sistemas, Universidade Federal de Pernambuco, 50740-530, Recife, Brazil. E-mail: barybin@mail.ru .*

Recent theoretical results obtained by Barybin and Santos [1] have suggested that the dynamic admittance of the $p-n$ -junction is proportional to the modified Bessel function of the first kind which depend on an amplitude of ac signal. This result extends the conventional theory usually encountered in known papers and textbooks. In this letter, some experimental results are presented to confirm our theoretical prediction. The measurements were performed with a lock-in amplifier, using a low noise operational amplifier. Two types of the $p-n$ -diodes were employed to check our theory: 1N914B diode, typically used for high-frequency applications, and 1N4007 diode, typically used in power supplies. Experimental results are consistent with the theoretical ones if a fitting parameter allowing for generation–recombination processes in the depletion layer is taken into account.

Keywords: $p-n$ -junction, dynamic admittance, diffusion conductance and capacitance, large signal.

I. INTRODUCTION TO THEORY

Recently Barybin and Santos [1] have applied a spectral approach to the theory of $p-n$ -junctions in order to take into account the effect of a large ac signal in a rigorous theoretical manner.

This approach is based on the general diffusion–drift equations for injected minority carriers, which is a standard practice for semiconductor electronics. The only specific feature distinguishing our approach from others is related to the initial representation of desired carrier concentrations in the form of Fourier expansion over frequency harmonics. Such harmonics are produced by nonlinear processes in $p-n$ -junctions when a sufficiently large ac voltage amplitude V_1 is applied to the junction together with the dc bias voltage V_0 . As a result, spectra of both the excess concentration of injected carriers and the external circuit current have been derived (see formulas (25), (26), and (32) of paper [1]). The use of appropriate terms in Fourier series has given rise to new expressions for the dc component J_0 and ac component J_1 of the external circuit current which determine the static current–voltage characteristic $J_0(V_0)$ and the dynamic admittance $Y = J_1/V_1$. They have both proved to be dependent not only on V_0 but also on V_1 , in the case of nonlinear (in ac signal) regime of operation of the $p-n$ -junction.

Below we shall experimentally verify the novel theoretical result concerning a dependence of the dynamic admittance on the amplitude of applied ac voltage $V_{\sim} = 2V_1$. This dependence was missed by other authors beginning with Shockley’s original papers [2, 3]. They all assume that the amplitude of the ac voltage is much smaller than V_T ($V_{\sim} \ll V_T \equiv \kappa T/q$). This approximation is also used in popular books such as [4, 5]. The basic model of a diode admittance is a parallel combination of the conductance G_d and capacitance C_d . Based on the old theory, the dynamic admittance of the $p-n$ -diode is derived in the form [4, 5]

$$Y(\omega) = G_d^{old}(\omega) + i\omega C_d^{old}(\omega) \quad (1)$$

with the following *old* expressions for the diffusion conductance and capacitance:

$$G_d^{old}(\omega) = \frac{\sqrt{1 + \sqrt{1 + \omega^2 \tau_p^2}}}{\sqrt{2}} G_{d0}, \quad (2)$$

$$C_d^{old}(\omega) = \frac{\sqrt{2}}{\sqrt{1 + \sqrt{1 + \omega^2 \tau_p^2}}} C_{d0}, \quad (3)$$

where τ_p is the minority carrier lifetime, and ω is an operating frequency of the applied ac voltage V_{\sim} . Expressions (2) and (3) are valid for the p^+-n -structures with a highly doped p -emitter when $p_n \gg n_p$ and the low-frequency diffusion conductance G_{d0} and capacitance C_{d0} are equal to [5]

$$G_{d0} = \frac{qS}{\kappa T} \frac{qD_p p_n}{L_p} \quad \text{and} \quad C_{d0} = \frac{qS}{\kappa T} \frac{qL_p p_n}{2}, \quad (4)$$

where $L_p = \sqrt{D_p \tau_p}$ is the diffusion length for holes with the equilibrium concentration p_n , and S is a cross-section area of the diode.

Considering the low injection theory and applying the spectral solution approach, we have found that for arbitrary applied voltage levels expressions (2) and (3) should be modified to the following *new* form (see Eqs. (48) and (49) of paper [1]):

$$G_d^{new}(\omega, V_\sim) = G_d^{old}(\omega) \frac{I_1(\beta V_\sim)}{\beta V_\sim/2}, \quad (5)$$

$$C_d^{new}(\omega, V_\sim) = C_d^{old}(\omega) \frac{I_1(\beta V_\sim)}{\beta V_\sim/2}, \quad (6)$$

so that instead of the old expression (1) for the dynamic admittance we have a new one:

$$Y(\omega, V_\sim) = G_d^{new}(\omega, V_\sim) + i\omega C_d^{new}(\omega, V_\sim). \quad (7)$$

As follows from these formulas, the new diffusion conductance and capacitance depend not only on the frequency ω given by the old formulas (2) and (3) but also on the ac voltage amplitude V_\sim appearing in the modified Bessel function of first order $I_1(\beta V_\sim)$, where $\beta = q/\kappa T$. In the low-frequency limit when $(\omega \tau_p)^2 \ll 1$, equations (2)–(3) and (5)–(6) reduce to the following normalized quantities:

$$\frac{G_d^{new}(0, V_\sim)}{G_{d0}} = \frac{C_d^{new}(0, V_\sim)}{C_{d0}} = \frac{I_1(\beta V_\sim)}{\beta V_\sim/2}. \quad (8)$$

At low signal amplitudes when $V_\sim \ll V_T$, the right-hand side of Eq. (8) is approximately equal to 1, which is the result usually found in the literature (see, e. g., formulas (64)–(66) and Fig. 23 of book [5]). Based on the new theory, even at zero bias it is possible to get experimental evidence of the dynamic behavior predicted by formula (8).

Our objective is to investigate a dependence of the new diffusion conductance on the ac voltage amplitude, $G_d^{new}(0, V_\sim)$, at low frequencies and zero bias. Although the diffusion capacitance $C_d^{new}(0, V_\sim)$ can also be measured, we shall not consider it here because at zero bias the total capacitance is dominated by the depletion capacitance. Below we present the experimental results obtained from conductance measurements to corroborate the new large-signal theory of p – n -junctions [1].

II. EXPERIMENTAL TECHNIQUE AND RESULTS

Our theory developed in paper [1] is based on the ideal Shockley model of the abrupt p – n -junction with neglecting generation–recombination processes in the depletion layer [3]. But in practice, such processes may be important for the actual p – n -diodes employed below in our experiment. So they have to be taken into account at least phenomenologically, as suggested by Sze [5]. Let us follow him and correct our theoretical results by an empirical factor n which is introduced so as to provide the following replacement:

$$\beta \equiv \frac{q}{\kappa T} \rightarrow \frac{q}{n\kappa T} \equiv \beta_n. \quad (9)$$

Values of the factor n lie between 1 and 2: $n = 1$ when a contribution of the generation–recombination processes is negligibly small, and $n = 2$ if the recombination current dominates over the diffusion one [5].

By using the replacement (9), expression (8) for the low-frequency dynamic conductance can be rewritten in the following corrected form:

$$G_d^{new}(0, V_\sim) = g_n(\beta V_\sim) G_{d0}, \quad (10)$$

where the correcting function $g_n(\beta V_\sim)$ is defined as

$$g_n(\beta V_\sim) = \frac{I_1(\beta_n V_\sim)}{\beta_n V_\sim/2} \equiv \frac{I_1(\beta V_\sim/n)}{\beta V_\sim/2n}. \quad (11)$$

In general, the modified quantity β_n in expression (11) takes into account not only a contribution from the generation–recombination processes by means of the factor n but also that from a priori unknown temperature T of a p – n -junction under experimental investigation. Hence, the product nT can be used as a fitting parameter to adjust the

theoretical relations (10)–(11) with experimental results obtained below. The correcting function $g_n(\beta V_{\sim})$ expressed by formula (11) is plotted in Fig. 1 for $T = 300$ K and five values of the fitting parameter $n = 1.0, 1.25, 1.5, 1.75$, and 2.0 .

To verify our theory, we built a simple apparatus using a dual-phase DSP lock-in amplifier, Stanford Research Systems model SR830, and a low noise electrometer grade operational amplifier, Burr-Brown OPA 128JM (see Fig. 2). The operational amplifier is in the inverter configuration. The ac voltage from the lock-in amplifier is directly applied to the diode with no bias, and the output of the amplifier is connected directly to the lock-in. The lock-in amplifier has two displays — X and Y which give the root-mean-square (rms) value of output signal at the excitation frequency ω . It is easy to show that the lock-in output in the X and Y displays is equal to

$$V_{out}^X = -RV_{in}[G_d(\omega) \cos(\phi - \phi_0) + \omega C_d(\omega) \sin(\phi - \phi_0)], \quad (12)$$

$$V_{out}^Y = -RV_{in}[G_d(\omega) \sin(\phi - \phi_0) + \omega C_d(\omega) \cos(\phi - \phi_0)]. \quad (13)$$

Here R is a feedback resistor, V_{in} is the rms value of the lock-in oscillator voltage ($V_{in} = V_{\sim}/\sqrt{2}$), ϕ is the internal phase of the lock-in oscillator signal connected to the phase detector, and ϕ_0 is the phase of the lock-in oscillator signal after passing through an external circuit. From Eqs. (12) and (13) it follows that the two displays are $\pi/2$ out of phase from each other.

To get correct experimental values, it is necessary to adjust a phase ϕ of the lock-in local oscillator so that the X-display would be used for the conductance voltage $|V_{out}^X| = RV_{in}G_d$ and the Y-display for the capacitance voltage $|V_{out}^Y| = RV_{in}\omega C_d$. As follows from expressions (12) and (13), it can be realized only if $\phi = \phi_0$. The phase ϕ is adjusted with a reference capacitor C which is placed between the local oscillator and the minus input of the operational amplifier instead of diode D , as shown in Fig. 2. The phase adjustment is carried out until zero voltage is observed in the conductance X-display, i. e., when $\phi = \phi_0$. Then Eqs. (12) and (13) yield the required results:

$$G_d(\omega, V_{\sim}) = \frac{1}{R} \left. \frac{|V_{out}^X|}{V_{in}} \right|_{\phi = \phi_0} \quad \text{and} \quad \omega C_d(\omega, V_{\sim}) = \frac{1}{R} \left. \frac{|V_{out}^Y|}{V_{in}} \right|_{\phi = \phi_0}. \quad (14)$$

After the adjustment, the reference capacitor C is replaced by a measured diode D and the measurements are performed by varying the applied ac voltage. The operating frequency of the lock-in internal oscillator was chosen 1 kHz to surely provide the relation $\omega\tau_p \ll 1$ underlying the initial theoretical expression (8). To extract the conductance, one must normalize the data.

For our experiments we have employed two different diodes — the 1N914B, a common high frequency diode, and the 1N4007, a diode used in power applications such as power supplies. All resistors and capacitors used in the experiment were measured with the Stanford Research Systems model SR720 LCR meter. The measurement error is found to be below 1%.

The experimental results for two above-mentioned diodes are presented in Figs. 3 and 4.

As seen from Eqs. (10) and (11), the low-voltage measurements (when $g_n = 1$) give values of the low-frequency diffusion conductance G_{d0} defined by formula (4). These values have proved to be equal $G_{d0} \simeq 6.4 \times 10^{-7}$ mho for the 1N914B diode and $G_{d0} \simeq 3.7 \times 10^{-7}$ mho for the 1N4007 diode.

From the experimental curves plotted in Figs. 3 and 4 it follows that the modified factor $\beta_n \equiv q/n\kappa T$ should be equal to 20.6 for the 1N914B diode and 20.1 for the 1N4007 diode in order to fit the theoretical expression (10). Hence, the fitting parameter nT is respectively equal to 560 K and 574 K, which for the operating temperature $T = 350$ K provides the following values of the generation–recombination factor $n = 1.6$ and $n = 1.64$. Therefore, both the diodes operate in a regime when the recombination current slightly dominates over the diffusion current.

III. CONCLUSION

Application of a spectral approach to the charge carrier transport in p - n -junctions with an arbitrary signal amplitude has allowed us to obtain new results which were previously lost by all the authors. Experimental results have corroborated theoretical predictions of our large-signal theory.

The authors would like to thank the CNPq (Brazilian agency) for its supporting this work. One of the authors (EJPS) would also like to thank the “Instituto do Milênio” program funded by the CNPq.

-
- [1] A. A. Barybin, and E. J. P. Santos, "Revision of large signal theory for $p-n$ -junctions", submitted for publication in IEEE Transactions on Electron Devices.
 - [2] W. Shockley, "The theory of $p-n$ -junctions in semiconductors and $p-n$ -junction transistors," *Bell Syst. Tech. J.*, vol. 28, p. 435, 1949.
 - [3] C. T. Sah, R. N. Noyce, and W. Shockley, "Carrier generation and recombination in $p-n$ -junctions and $p-n$ -junction characteristics," *Proc. IRE*, vol. 45, p. 1228, 1957.
 - [4] R. A. Smith, *Semiconductors*, 2nd ed., London: Cambridge University Press, 1979.
 - [5] S. M. Sze, *Physics of Semiconductor Devices*, 2nd ed., New York: Wiley, 1981.

Figure captions

Fig. 1. The correcting function $g_n(\beta V_\infty)$ defined by formula (11) and calculated for $T = 300K$ and five values of the fitting parameter $n = 1.0$ (curve 1), 1.25 (curve 2), 1.5 (curve 3), 1.75 (curve 4), and 2.0 (curve 5).

Fig. 2. Experimental setup with a measured diode D whose dynamic admittance $Y(\omega, V_\infty)$ is given by formula (7).

Fig. 3. Theoretical curve and experimental data for the 1N914B diode.

Fig. 4. Theoretical curve and experimental data for the 1N4007 diode.

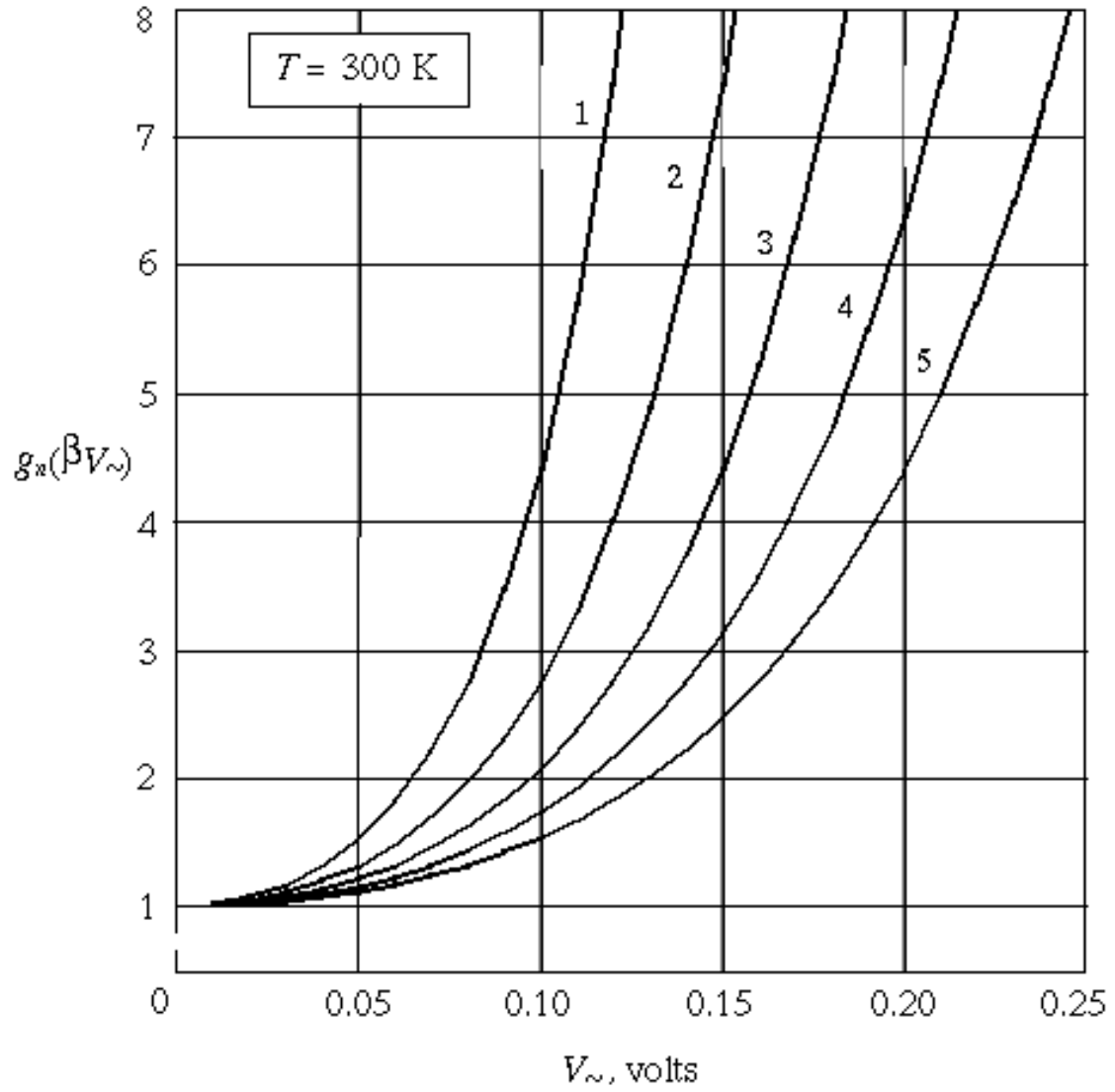


Fig .1 - Santos and Barybin

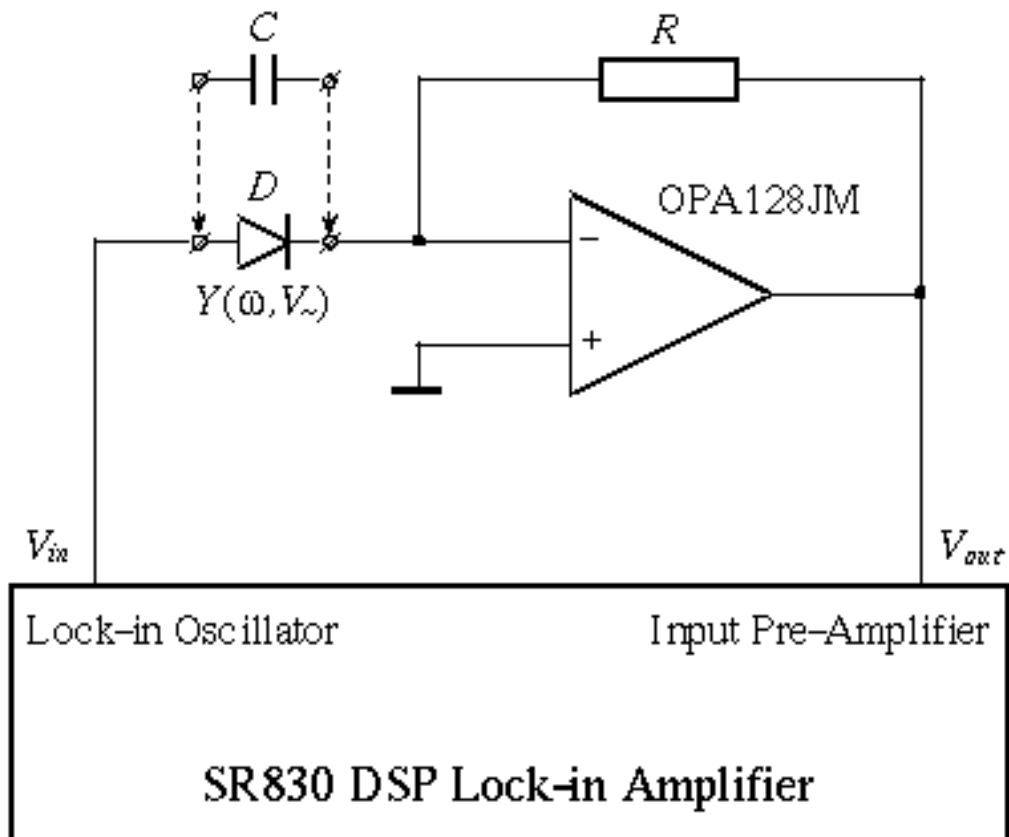


Fig .2 - Santos and Barybin

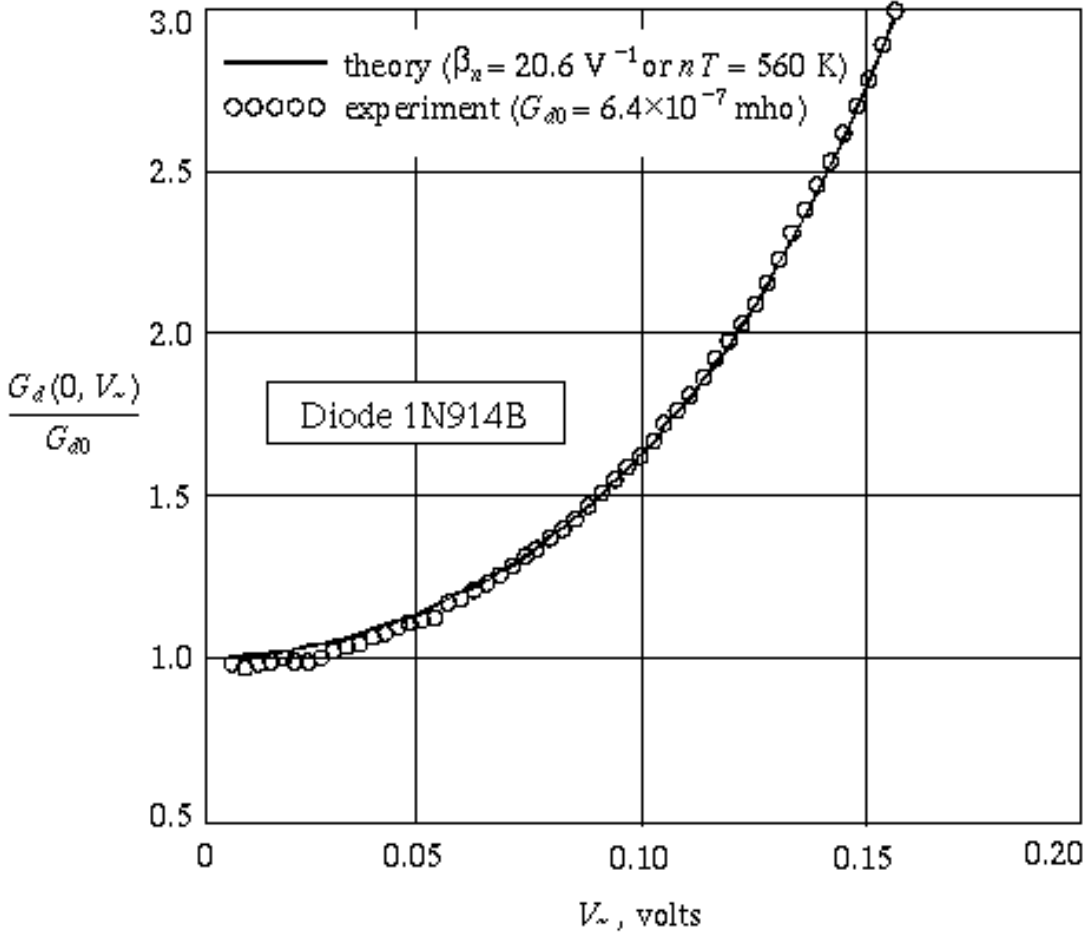


Fig .3 - Santos and Barybin

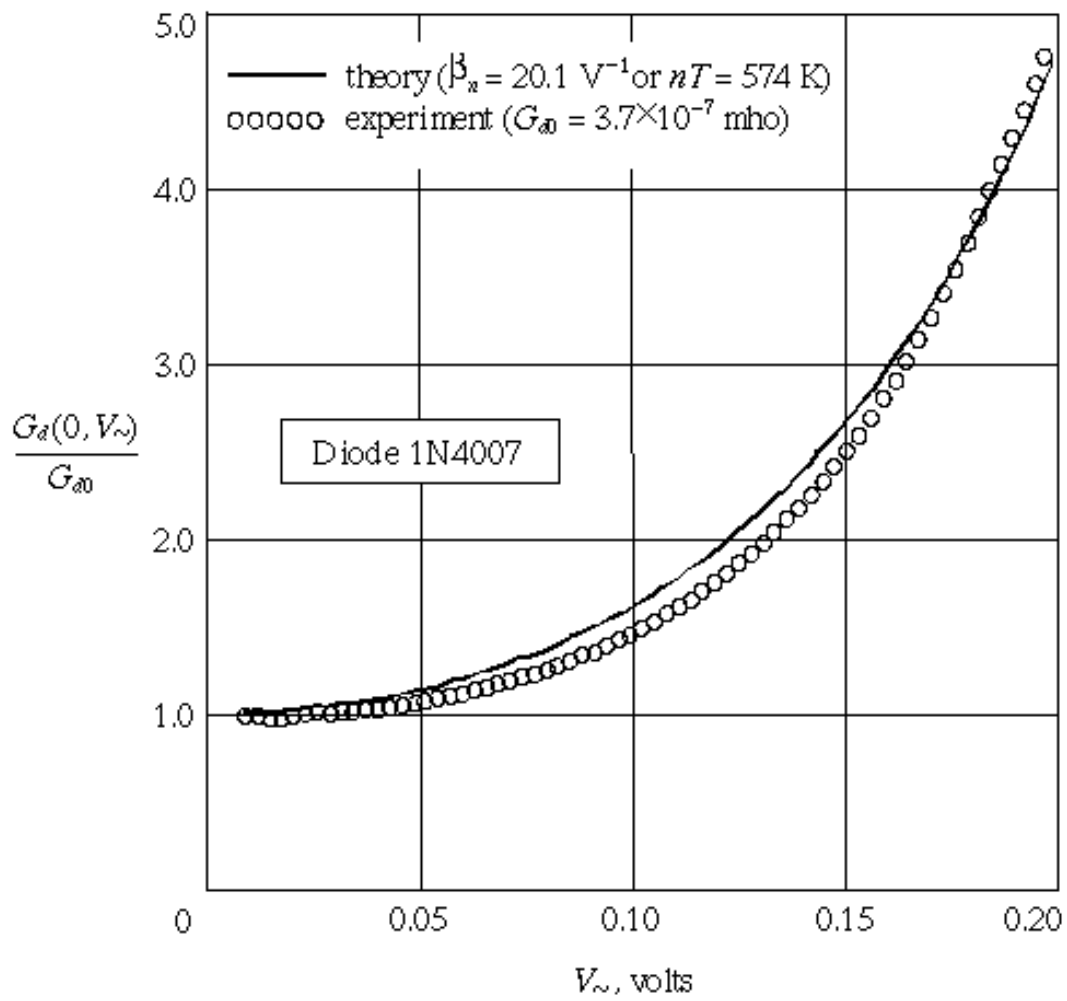


Fig .4 - Santos and Barybin